Journal of the Optical Society of America B

OPTICAL PHYSICS

Analytical description of resonances in Fabry–Perot and whispering gallery mode resonators

Aigars Atvars

Photonics Laboratory, Institute of Astronomy, University of Latvia, Raina bulvaris 19, Riga, LV-1586, Latvia (Aigars.Atvars@lu.lv)

Received 11 February 2021; revised 31 August 2021; accepted 7 September 2021; posted 7 September 2021 (Doc. ID 419993); published 29 September 2021

Whispering gallery mode optical resonators have attracted attention due to their simplicity and applicability for sensing. In this paper, analytical formulas are provided that describe resonance conditions in optical resonators. Basic terms (resonance wavelengths and frequencies, free spectral range, *Q*-factor, summation principle of *Q*-factors of various processes, finesse, etc.) are introduced. A description of interference of an infinite number of waves of progressively smaller amplitudes and equal phase differences is given. A description of a Fabry–Perot resonator with nonequal reflection coefficients is also given as well as analysis of all-pass and add-drop optical filters. The presented description of resonators will help to analyze the effects of optical resonators, interpret the results of experiments, and guide the development of novel applications of microresonators.

https://doi.org/10.1364/JOSAB.419993

1. INTRODUCTION

Optical whispering gallery mode resonators (WGMRs) [1] are optical structures that confine light due to total internal reflection. Their properties have attracted significant attention in the last decade [2,3]. Different WGMRs allow the application of variable experimental conditions to change their internal properties [4,5]. Most studied WGMRs 3D structures are balls [6], toroids [7], and 2D structures, i.e., rings [8]. The light is introduced in these structures most often by a prism [9] or tapered fiber coupling [10]. These resonators are outstanding because they form optical resonances with high Q-factors up to $10^7 - 10^{10}$ [11,12]. When the external environment, e.g., temperature [13], humidity [14], or refractive index [15], changes, the resonances shift; therefore, WGMRs are usable as sensors to monitor these changes [16]. In biosensing, WGMRs are used as units where tested molecules stick to their surface [17,18]. Another significant aspect of WGMRs is a high density of light confined in these structures, thus forming conditions for studies of nonlinear optical effects [19]. For example, whispering gallery mode frequency combs [20] are formed through such effects.

While most of the studies in this field are concentrated on the particular peculiarities and application issues of WGMR, there is a lack of a detailed description of the theoretical aspects of these resonators. In this paper, we provide the advanced classical analytical description of optical resonances with mentioning only some results obtained via Maxwell's equations (ME) [21,22]. This gives space to accent physical processes operated in resonators, e.g., interference of waves, and not to dive into ME formalism, which gives more precise results of resonances but is ambiguous and practically usable only in some general resonator geometries, e.g., balls and cylinders. Formulas provided here give a basic level of deep understanding of resonances of optical resonators, including WGMR and Fabry–Perot resonators. Finite element simulations of WGMRs and light propagation in them can be made, for example, in COMSOL Multiphysics software and can be used as a supplementary material to analytical theory [23–26].

This paper contains the description of the main parameters of optical resonances such as resonance wavelengths and frequencies, free spectral range, Q-factor, summation principle of Q-factors of various processes, finesse, etc. The intensity distribution of resonance spectra is derived from the interference of an infinite number of waves of smaller amplitudes and equal phase differences. Resonances of Fabry–Perot resonators with different and equal reflection coefficients of their mirrors are described. Their similarity to resonances of whispering gallery mode resonators with single and two waveguides coupling is presented. Provided formulas with underlying proofs form a concept system for an in-depth understanding of the formation of optical resonances.

2. BASIC ANALYTICAL FORMULAS FOR RESONATOR DESCRIPTION

Optical resonances observed in WGMR can be described by wavelength positions λ_i and widths $\Delta\lambda_i$ or frequency positions

ν_i and widths $\Delta\nu_i$. The whole spectra can be expressed as $I(\lambda)$ or $I(\nu)$.

A. Wavelength in Media

Resonance frequency ν_i is the same across various media. However, a resonance wavelength inside the resonator λ_{mat} differs from the wavelength in vacuum λ_{vac} as

$$\lambda_{\text{mat}} = \frac{\lambda_{\text{vac}}}{n}, \quad (1)$$

where n is a refractive index of media where light propagates. Further, we will describe resonances as wavelengths in vacuum $\lambda = \lambda_{\text{vac}}$.

B. Resonance Positions

A resonance condition appears when light interferes positively. If two waves have phases ϕ_1 and ϕ_2, respectively, the resonance condition is

$$e^{i\phi_2} = e^{i\phi_1}, \quad (2)$$

and more specifically,

$$\phi_2 - \phi_1 = \pm 2\pi m, \quad (3)$$

where m is a whole number. Generally, for monochromatic wave $\phi = \omega t - kx + \Delta\phi$, where ω is frequency, t is time, k is the wavenumber, x is the propagation axis, and $\Delta\phi$ is a phase shift introduced, for example, by the reflection of a wave. If wave 2 is originated from wave 1, both waves have the same frequency ω; further, when no additional phase shift is obtained due to reflections, and the position difference in the x axis is L, then $\phi_2 - \phi_1 = -kL$, where $k = 2\pi n/\lambda_m$, n is a refractive index of the media of a wave propagation, and λ_m is a wavelength. As wavelength and path length L are positive, Eq. (3) turns into

$$\lambda_m = nL \cdot \frac{1}{m}. \quad (4)$$

The same equation can be obtained by stating that a resonance condition is formed when the length L of the light path loop in an optical structure with the refractive index n is equal to positive natural number m of wavelength λ_m in this media.

The corresponding resonance frequency for index m is

$$\nu_m = \frac{c}{nL} \cdot m. \quad (5)$$

The maximal resonance wavelength is equal to light path L multiplied by a refractive index (when $m = 1$):

$$(\lambda_m)_{\max} = L \cdot n. \quad (6)$$

The minimal resonance frequency is

$$(\nu_m)_{\min} = \frac{c}{nL}. \quad (7)$$

If path L is a circle with a radius a, then resonance conditions are

$$\lambda_m = 2\pi a n \cdot \frac{1}{m}, \quad (8)$$

$$\nu_m = \frac{c}{2\pi a n} \cdot m. \quad (9)$$

In the first approximation, for circular or spherical whispering gallery mode resonators, a is equal to the radius r_o of a circle or a sphere. In an advanced approximation, a is smaller than the radius of the sphere by the fraction of a wavelength as the light travels inside the resonator, and the resonance condition differs slightly for TE and TM modes. For example, for spherical resonators, their resonance positions derived from Maxwell's equations [27,28] are

$$\nu_m = \frac{c}{2\pi r_0 n} \cdot \left[\begin{array}{l} m + \frac{1}{2} + 2^{-1/3}\alpha(m_r)\left(m+\frac{1}{2}\right)^{1/3} \\ -\frac{P}{(n_r^2-1)^{1/2}} + \frac{3}{10}2^{-2/3}\alpha^2(m_r)\left(m+\frac{1}{2}\right)^{-1/3} \\ -2^{-1/3}P\left(n_r^2 - \frac{2}{3}P^2\right)\frac{\alpha(m_r)\left(m+\frac{1}{2}\right)^{-2/3}}{(n_r^2-1)^{3/2}} \end{array} \right], \quad (10)$$

where effective refractive index $n_r = n/n_2$, n_2 is the refractive index of the media surrounding the resonator, $P = n_r$ in TE mode and $P = 1/n_r$ in TM mode, $\alpha(m_r)$ is the position of the m_rth root of the Airy function $Ai(-\alpha)$, and m_r is the radial mode number.

For the first radial TE mode, $m_r = 1$ and $\alpha(1) = 2.33811$. When $m \gg 1$ and the resonator is surrounded by air $n_2 = 1$, the resonance position in Eq. (10) turns into [1]

$$\nu_m = \frac{c}{2\pi r_0 n} \cdot \left(m + 1.856 m^{1/3} + \frac{1}{2} - \frac{n}{\sqrt{n^2-1}} \right). \quad (11)$$

For typical microresonators and experimental conditions $r_0 \approx 0.5$ mm, $n \approx 1.45$ (fused silica), and $\lambda_m \approx 780$ nm. From Eq. (9), we obtain $m \approx 6040$, assuming $a = r_0$. Correspondingly, Eq. (11) gives $m \approx 6007$. This means that the correction of resonance positions derived from Maxwell's equation gives the shift of resonances by about 33 modes compared with Eq. (9) when a is used as a radius of the resonator. Equation (9) can also be used in advanced models of resonances. Then, to keep the simplicity of the resonance condition, typically advanced corrections are hidden inside the parameter of effective radius a, which is nontrivial to derive, and the effective refractive index n in the simplest case is n_r, as described in Eq. (10).

In the case when refractive index n is nonhomogenous in a media, the resonance condition in Eq. (4) turns into

$$\lambda_m = \frac{1}{m} \oint_L n_L \mathrm{d}L, \quad (12)$$

where n_L is a refractive index within a specific step dL. Evanescent interaction of waves can be hidden in n_L.

C. Free Spectral Range

The distance between the two closest resonances is called the "free spectra range" (FSR).

For wavelength scale, the FSR is

$$\text{FSR}(\lambda_m) = \lambda_{m+1} - \lambda_m = -\frac{\lambda_m^2}{(nL + \lambda_m)} \approx -\frac{\lambda_m^2}{nL}, \quad (13)$$

which means that peaks are not equidistant. We assumed that $nL \gg \lambda_m$, which is valid for large resonators.

In frequency scale, the FSR is

$$\mathrm{FSR}\,(\nu_m) = \nu_{m+1} - \nu_m = \frac{c}{nL}, \tag{14}$$

which means equidistant resonances.

D. Quality Factor

Quality factor of the resonator system is defined as [29,30]

$$Q = 2\pi \frac{\text{stored energy}}{\text{energy loss per oscillation period}}. \tag{15}$$

Stored energy in the resonator is proportional to the light intensity I_0 in the resonator. Due to energy dissipation, which is characterized by the decay time τ, the light intensity I in the resonator decays in time t according to

$$I = I_0 e^{-t/\tau}. \tag{16}$$

After one oscillation period $T = 1/\nu$, the intensity turns into

$$I = I_0 e^{-T/\tau} = I_0 e^{-1/(\tau\nu)}. \tag{17}$$

Correspondingly, Eq. (15) becomes

$$Q = 2\pi \frac{1}{1 - e^{-1/(\tau\nu)}}. \tag{18}$$

Assuming the decay to be slow so that $1/(\tau\nu) \ll 1$, Eq. (18) turns into

$$Q = 2\pi\nu\tau = \tau\omega, \tag{19}$$

which is an alternative definition of Q-factor. Lifetime τ of a resonator can be measured experimentally [12], thus deriving the Q-factor of the resonator system.

Let us analyze the case when the amplitude $U(t)$ of the optical signal oscillates in time t with an angular frequency ω_o. It is related to its intensity as $I(t) \sim U(t)^2$. When the intensity $I(t)$ of the optical signal decays according to Eq. (16), we obtain $U(t) = U_0 e^{-\frac{t}{2\tau}} e^{i\omega_0 t}$, where U_0 is a coefficient. By taking the Fourier transform, we obtain

$$\begin{aligned} U(\omega) &= \frac{1}{2\pi}\int_0^{+\infty} U(t) e^{-i\omega t}\mathrm{d}t \\ &= \frac{U_0}{2\pi i} \frac{\frac{1}{2\tau} - i(\omega - \omega_0)}{\left(\frac{1}{2\tau}\right)^2 + (\omega - \omega_0)^2}. \end{aligned} \tag{20}$$

Now the light intensity $I(\omega)$ in an angular frequency scale becomes

$$I(w) \sim U(\omega)^2 \sim \frac{1}{\left(\frac{1}{2\tau}\right)^2 + (\omega - \omega_0)^2}. \tag{21}$$

The maximal signal appears when $\omega = \omega_0$. The full width of the signal $I(\omega)$ at half maximum (FWHM) appears to be

$$\Delta\omega = \frac{1}{\tau}. \tag{22}$$

In a frequency and wavelength scale, the FWHM becomes

$$\Delta\nu = \frac{1}{2\pi\tau}, \tag{23}$$

$$\Delta\lambda = \frac{\lambda^2}{2\pi c\tau}. \tag{24}$$

According to Eqs. (19), (22), (23), and (24), the Q-factor can be expressed as

$$Q = \frac{\omega}{\Delta\omega} = \frac{\nu}{\Delta\nu} = \frac{\lambda}{\Delta\lambda}. \tag{25}$$

The exponential behavior of the decay of light intensity in the resonator, as expressed in Eq. (16), can be derived from processes that initiate the loss dI of the intensity I, which is proportional to the value of this intensity and time interval dt as $dI \sim -Idt$. In the case of many decay factors described by decay rates $a_1, a_2, a_3, \ldots$, the intensity loss is described as

$$\begin{aligned} dI &= -a_1 I dt - a_2 I dt - a_3 I dt - \ldots \\ &= -I(a_1 + a_2 + a_3 + \ldots)\, dt. \end{aligned} \tag{26}$$

After integration, we obtain

$$I = I_0 e^{-(a_1+a_2+a_3+\ldots)t}, \tag{27}$$

where I_0 is the intensity of the signal at $t = 0$. Based on Eqs. (16) and (19), each decay factor a_i can be described by $1/Q_i = a_i/\omega$, where i is the index of the factor. Thus,

$$I = I_0 e^{-(1/Q_1+1/Q_2+1/Q_3+\ldots)\omega t} = I_0 e^{-(1/Q)\omega t}. \tag{28}$$

And

$$\frac{1}{Q} = \frac{1}{Q_1} + \frac{1}{Q_2} + \frac{1}{Q_3} + \ldots \tag{29}$$

This shows that the total Q-factor Q of the system can be expanded by various sub-Q-factors Q_i initiated by various decay processes [12].

E. Finesse

Finesse $\mathcal{F}$ describes the resonator and is defined as the FSR divided by the full width of resonance at the half maximum (FWHM):

$$\mathcal{F} = \frac{\mathrm{FSR}}{(\mathrm{FWHM})}. \tag{30}$$

Taking into account Eqs. (14), (19), and (23), we obtain

$$\mathcal{F} = \frac{c}{nL\Delta\nu} = \frac{2\pi\tau c}{nL} = \frac{Qc}{nL\nu} \tag{31}$$

and

$$Q = \mathcal{F}\frac{nL\nu}{c} = \mathcal{F}\frac{L}{(\lambda/n)}. \tag{32}$$

Here, we see that the Q-factor is equal to the finesse when light path loop length L equals the wavelength in the optical structure. If the resonance is formed by several wavelengths in the light path loop length, then the Q-factor is larger than the finesse.

For the resonance condition in Eq. (4), Eq. (32) turns into

$$Q = \mathcal{F} m, \tag{33}$$

where m is the number of wavelengths within the light path loop L.

F. Intensity Distribution of a Resonance Spectra

Let us examine the interference of an infinite number of waves of progressively smaller amplitudes U_i and equal phase differences [29], where i is the index of the wave changing from 1 to infinity. The first wave has the intensity I_0 and an amplitude $U_1 = \sqrt{I_0}$. The next wave is smaller by the factor of $h = |h|e^{i\phi}$, $|h| < 1$, compared with the previous wave, and incorporates the decay of the amplitude and a phase shift ϕ. Thus, a series of waves is formed:

$$U_1,\ U_2 = hU_1,\ U_3 = hU_2 = h^2 U_1, \ldots \tag{34}$$

The summary field amplitude is

$$\begin{aligned} U &= U_1 + U_2 + U_3 + \ldots \\ &= U_1\left(1 + h + h^2 + h^3 + \ldots\right) = U_1 \sum_{k=0}^{\infty} h^k \\ &= \frac{U_1}{1-h} = \frac{\sqrt{I_0}}{1-|h|e^{i\phi}}. \end{aligned} \tag{35}$$

The total intensity is

$$I = |U|^2 = \frac{I_0}{|1-|h|e^{i\phi}|^2} = \frac{I_0}{1+|h|^2 - 2|h|\cos\phi}. \tag{36}$$

This formula can be rewritten in a form that better describes its resonance behavior

$$I = \frac{I_0}{(1-|h|)^2 + 4|h|\sin^2(\phi/2)}. \tag{37}$$

The maximal and minimal values of the intensity are

$$I_{\max} = \frac{I_0}{(1-|h|)^2}, \tag{38}$$

$$I_{\min} = \frac{I_0}{(1+|h|)^2}. \tag{39}$$

The intensity in Eq. (37) can be rewritten as

$$I = \frac{I_{\max}}{1 + \left((2\sqrt{|h|})/1-|h|\right)^2 \sin^2(\phi/2)}. \tag{40}$$

The resonance depth I_{res} is

$$I_{\mathrm{res}} = I_{\max} - I_{\min} = \frac{4|h|I_0}{(1-|h|^2)^2}, \tag{41}$$

and can be characterized by coefficients K_1 and K_2:

$$I_{\mathrm{res}} = K_1 \cdot I_{\max} = K_2 \cdot I_0, \tag{42}$$

$$K_1 = \frac{4|h|}{(1+|h|)^2}, \tag{43}$$

$$K_2 = \frac{4|h|}{\left(1-|h|^2\right)^2}. \tag{44}$$

According to Eq. (40), the resonance FWHM in a phase scale ϕ is

$$\Delta\phi = 4\arcsin\frac{1-|h|}{2\sqrt{|h|}}. \tag{45}$$

For the WGMR case, ϕ is a phase shift that is experienced by the light, when it travels light path loop distance L in a media with refractive index n:

$$\phi = k \cdot L = \frac{2\pi n}{\lambda} \cdot L = \frac{2\pi n L}{c} \cdot \nu. \tag{46}$$

Then,

$$I = \frac{I_0}{(1-|h|)^2 + 4|h|\sin^2\left(\frac{\pi n L}{\lambda}\right)}. \tag{47}$$

In frequency scale,

$$I = \frac{I_0}{(1-|h|)^2 + 4|h|\sin^2\left(\frac{\pi n L}{c}\nu\right)}. \tag{48}$$

If we assume $|h|$ to be fixed and ν to be variable, then the maximal value of intensity is achieved when $\sin(\frac{\pi n L}{c}\nu) = 0$, thus giving the resonance condition

$$\frac{\pi n L}{c}\nu_m = \pi m, \tag{49}$$

where m is a positive natural number as $\nu_m > 0$. Resonance condition

$$\nu_m = \frac{c}{nL} \cdot m \tag{50}$$

is equal to Eq. (5) as expected.

Full width at half maximum $\Delta\nu$ of the intensity in Eq. (48) is obtained from equation

$$(1-|h|)^2 = 4|h|\sin^2\left(\pi n L\left(\nu_m + \Delta\nu/2\right)/c\right). \tag{51}$$

Taking into account the identity in Eq. (49), we obtain

$$\Delta\nu = \frac{2c}{\pi n L}\arcsin\frac{1-|h|}{2\sqrt{|h|}}. \tag{52}$$

If we make a similar procedure for Eq. (47), then

$$(1-|h|)^2 = 4|h|\sin^2\left(\frac{\pi n L}{\lambda_m + \Delta\lambda/2}\right), \tag{53}$$

$$\frac{\pi n L}{\lambda_m} = \pi m, \tag{54}$$

$$\frac{\pi n L}{\lambda_m + \Delta\lambda/2} = \arcsin\frac{1-|h|}{2\sqrt{|h|}} + \pi m, \tag{55}$$

$$\Delta\lambda = \frac{2\lambda_m \arcsin\frac{1-|h|}{2\sqrt{|h|}}}{\arcsin\frac{1-|h|}{2\sqrt{|h|}} + \pi m} \tag{56}$$

$$\approx \frac{2\lambda_m^2}{\pi n L}\arcsin\frac{1-|h|}{2\sqrt{|h|}} \tag{57}$$

$$\approx \frac{2\lambda^2}{\pi n L}\arcsin\frac{1-|h|}{2\sqrt{|h|}}, \tag{58}$$

for cases when $m \gg 1$ as $|\arcsin(x)| \leq \pi/2$ for all values of parameter x.

Thus, Q-factor is obtained as

$$Q = \frac{\pi n L \nu}{2c}\arcsin^{-1}\frac{1-|h|}{2\sqrt{|h|}}. \tag{59}$$

Equation (48) shows the same maximal intensities for each of the resonances if decay rates $|h|$ are the same for all frequencies. If $|h|$ depends on ν, then resonances with various intensities can be obtained.

$|h|$ can be expressed as

$$|h| = e^{-\beta} = e^{-t_0/(2\tau)} = e^{-nL/(2c\tau)} = e^{-\pi n L \nu/(cQ)}, \tag{60}$$

where t_0 is time for the signal to travel one loop with path distance L, and τ is the decay rate of the intensity as given by Eq. (16). Thus, Eq. (48) turns into

$$I = \frac{I_0}{\left(1-e^{-\frac{nL}{2c\tau}}\right)^2 + 4e^{-\frac{nL}{2c\tau}}\sin^2\left(\frac{\pi n L}{c}\nu\right)} \tag{61}$$

$$= \frac{I_0}{\left(1-e^{-\frac{\pi n L\nu}{cQ}}\right)^2 + 4e^{-\frac{\pi n L \nu}{cQ}}\sin^2\left(\frac{\pi n L}{c}\nu\right)}. \tag{62}$$

For slow decay $(1-|h|) \ll 1$, $|h| \approx 1 - t_0/(2\tau) = 1 - nL/(2c\tau)$, and the resonance width in Eqs. (52) and (58) and the Q-factor in Eq. (59) can be approximated as

$$\Delta\nu \approx \frac{c}{\pi n L}\frac{1-|h|}{\sqrt{|h|}} \approx \frac{c}{\pi n L}(1-|h|) \approx \frac{1}{2\pi\tau}, \tag{63}$$

$$\Delta\lambda \approx \frac{\lambda^2}{\pi n L}\frac{1-|h|}{\sqrt{|h|}} \approx \frac{\lambda^2}{\pi n L}(1-|h|) \approx \frac{\lambda^2}{2\pi c\tau}, \tag{64}$$

$$Q \approx \frac{\pi n L \nu}{c}\frac{\sqrt{|h|}}{1-|h|} \approx 2\pi\tau\nu, \tag{65}$$

as expected from Eqs. (23), (24), and (19).

For slow decay, Eqs. (61) and (62) turn into

$$I \approx \frac{I_0}{\left(\frac{nL}{2c\tau}\right)^2 + 4\sin^2\left(\frac{\pi n L}{c}\nu\right)} \tag{66}$$

$$\approx \frac{I_0}{\left(\frac{\pi n L \nu}{cQ}\right)^2 + 4\sin^2\left(\frac{\pi n L}{c}\nu\right)}. \tag{67}$$

When searched now for resonance width at half maximum $\Delta\nu$ close to resonance, we obtain $\nu/Q \approx \Delta\nu$, which is equal to Eq. (25).

By combining Eqs. (30), (14), and (63), we obtain

$$\mathcal{F} \approx \frac{\pi\sqrt{|h|}}{1-|h|} \approx \frac{\pi}{1-|h|} \approx \frac{2\pi c\tau}{nL}. \tag{68}$$

Now Eq. (47) can be rewritten as

$$I = \frac{I_{\max}}{1 + (2\mathcal{F}/\pi)^2\sin^2\left(\frac{\pi n L}{c}\nu\right)}, \tag{69}$$

$$I_{\max} = \frac{I_0}{(1-|h|)^2}. \tag{70}$$

The intensity in Eq. (69) takes the maximum value $I_{\max}$ when $\sin^2(\pi n L \nu/c) = 0$ and minimal value $I_{\min}$ when $\sin^2(\pi n L\nu/c) = 1$. Thus,

$$I_{\min} = \frac{I_{\max}}{1 + (2\mathcal{F}/\pi)^2}. \tag{71}$$

The resonance depth becomes

$$I_{\mathrm{res}} = I_{\max} - I_{\min} = K_1 \cdot I_{\max} = K_2 \cdot I_0, \tag{72}$$

$$K_1 = \frac{1}{1 + (\pi/(2\mathcal{F}))^2}, \tag{73}$$

$$K_2 = \frac{1}{(1-|h|)^2}\cdot\frac{1}{1+(\pi/(2\mathcal{F}))^2}, \tag{74}$$

$$I_{\mathrm{res}} = \frac{I_0}{(1-|h|)^2}\cdot\frac{1}{1+(\pi/(2\mathcal{F}))^2}. \tag{75}$$

For slow decay ($|h| \approx 1$), according to Eq. (68), the finesse becomes $\mathcal{F} \gg 1$ and

$$K_1 \approx 1 - (\pi/(2\mathcal{F}))^2 \approx 1, \tag{76}$$

$$K_2 \approx (\mathcal{F}/\pi)^2\frac{1}{1+(\pi/(2\mathcal{F}))^2} \approx (\mathcal{F}/\pi)^2. \tag{77}$$

It should be noted that, according to Eq. (70), $I_{\max}$ can reach infinity if there is no decay ($|h| = 1$). In this case, equations describe a situation when an infinite number of identical light fields are summarized; therefore, infinite summary intensity is a logical conclusion.

Close to resonance described by ϕ_{res} [see Eq. (46)] or ν_{res}, the intensity distribution in Eq. (69) becomes Lorentzian:

$$I = \frac{I_{\max}}{1 + (\mathcal{F}/\pi)^2(\phi - \phi_{\mathrm{res}})^2} \tag{78}$$

$$= \frac{I_{\max}}{1 + (2nL\mathcal{F}/c)^2(\nu - \nu_{\mathrm{res}})^2}. \tag{79}$$

G. Resonance Shift

The advantage of optical resonators is ease of use for sensing applications [16]. The most used mechanism that realizes the sensing process is the shift of resonance positions when the external environment, e.g., temperature, changes. This is realized by the expansion of the resonator and the change of its refractive index, as resonance positions depend on the light path length and refractive index [see Eq. (4)].

Thermal expansion of materials is described by the coefficient of thermal expansion α_0. For material with length L, the expansion dL for the temperature change dT is described as

$$\frac{dL}{dT} = \alpha_0 \cdot L. \tag{80}$$

The change of refractive index by a temperature is described by the thermo-optical effect and corresponding thermo-optical coefficient β_0 of a material:

$$\frac{dn}{dT} = \beta_0 \cdot n. \tag{81}$$

When both of these effects appear, then the resonance peak λ_m described by Eq. (4) shifts as

$$\frac{d\lambda_m}{dT} = \left(\frac{dn}{dT}L + n\frac{dL}{dT}\right) \cdot \frac{1}{m} = (\alpha_0 + \beta_0)\, nL \cdot \frac{1}{m}, \tag{82}$$

$$\frac{d\lambda_m}{dT} = \lambda_m (\alpha_0 + \beta_0), \tag{83}$$

and in frequency scale

$$\frac{d\nu_m}{dT} = -\nu_m (\alpha_0 + \beta_0). \tag{84}$$

For fused silica, $\alpha_0 = 0.55 \cdot 10^{-6}$ 1/K [31] and $\beta_0 = 11.3 \cdot 10^{-6}$ 1/K [32], thus showing that the thermo-optical effect is the main contributor to a resonance shift. Other effects may cause the shift of frequencies, for example, when additional substance appears in the path of light and when the volume of the media increases due to external humidity as in the case of glycerol [14]. The effect of the resonance shift due to changes in the environment allows us to use resonators as sensors.

3. ADVANCED ANALYTICAL FORMULAS FOR RESONANCE DESCRIPTION

A. Fabry–Perot Resonator

The Fabry–Perot resonator is an optical system with two parallel semitransparent mirrors placed at a distance $d = L/2$. Laser light is irradiated on one of the mirrors, and transmitted light of the whole system is measured [33,34]. There are two main types of Fabry–Perot resonators, i.e., bulk glass with parallel surfaces that are covered with reflection coatings [FP Type—1, Fig. 1(a)] and air-spaced plain parallel surfaces, which are covered with reflecting coatings on inner surfaces and with antireflecting coatings on outer surfaces [FP Type—2, Fig. 1(b)].

Let us derive a significant property of transmitted and reflected light that falls on the boundary of two optical medias. We suppose that incident light has amplitude a and is transmitted from media with refractive index n_1 to media with refractive index n_2 (Fig. 2). The amplitude of the ray in the second media becomes at, where t is the transmittance coefficient. The amplitude of the reflected ray is ar, where r is the reflectance coefficient. The time-reversal principle can be used, i.e., when the direction of light propagation changes to the opposite, the amplitudes of the field have to remain the same. Let us use r' as the reflection coefficient when the ray comes from media n_2 and reflects from media with n_1, and t' is the corresponding transmittance coefficient. Then, the time-reversal gives ray at to reflect as atr' and to be transmitted as att' and ray ar to be transmitted as art and reflected as ar^2 [see Fig. 2(b)]. Thus, we have

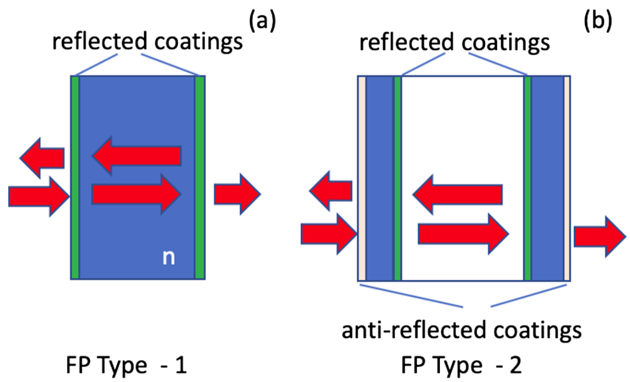

Fig. 1. Types of Fabry–Perot resonators: (a) solid etalon (Type 1); (b) air-spaced plain parallel surfaces (Type 2).

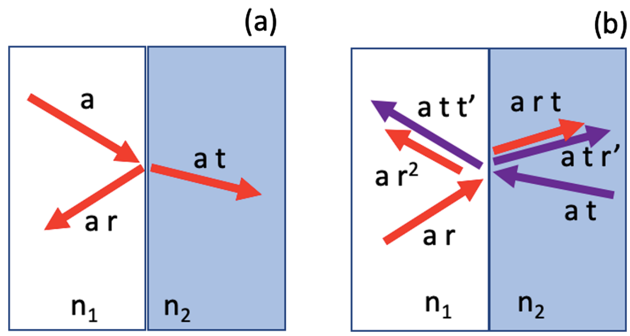

Fig. 2. (a) Scheme of directions of incident, reflected, and transmitted field rays when light is irradiated on the boundary between medias with different refractive indexes n_1 and n_2. (b) Scheme for comparison of incident, reflected, and transmitted fields with rays in time-reversal situation. The light propagates along one horizontal axis. Only for visualization purposes, rays have angles to the boundary that separates medias.

$$a = att' + ar^2, \tag{85}$$

$$0 = art + atr', \tag{86}$$

and

$$r^2 + tt' = 1, \tag{87}$$

$$t = t' = \sqrt{1 - r^2}, \tag{88}$$

$$r = -r'. \tag{89}$$

When both media are equal, then there is no reflected ray; thus, $r = r' = 0$ and $t = t' = 1$.

The reflection coefficient of the mirror (or semitransparent mirror) is assumed to be R, and it describes the proportion of intensity that is reflected. For the amplitude, this becomes $r = \sqrt{R}$ and $r' = -\sqrt{R}$ with r used when the ray reflects from media with a larger refractive index and r' used when the ray reflects from media with a smaller refractive index. In the second case, it can be described as a reflection with a coefficient r and a phase shift π. The transmission coefficient of light intensity is defined as $T = 1 - R$. For amplitude transmission, it becomes $t = t' = \sqrt{T}$.

Let us explore the Fabry–Perot resonator of Type 1 [Fig. 1(a)]. The resonator is filled with media with refractive coefficient n. The resonance condition appears when the distance between both mirrors is equal to positive natural number m of half wavelength:

$$d = \left(\frac{\lambda_m}{2n}\right) \cdot m, \tag{90}$$

$$\lambda_m = 2nd \cdot \frac{1}{m} = nL \cdot \frac{1}{m}, \tag{91}$$

which is equivalent to Eq. (4). In the same way, the equivalence will be found for resonance positions in frequency scale and in the FSR.

The left reflective layer (first mirror) of the Fabry–Perot resonator (see Fig. 3) is characterized by the intensity reflection coefficient R_1, transmittance coefficient T_1, corresponding amplitude reflection coefficient $r_1 = \sqrt{R_1}$, and transmittance coefficient $t_1 = \sqrt{T_1}$. The right reflective layer (second mirror) is characterized similarly by coefficients R_2, T_2, r_2, and t_2. The incident light with intensity I_0 and field amplitude $U_0 = \sqrt{I_0}$ travels from left to right and hits the left side of the resonator. This field is transmitted through the first mirror as $U_{01} = t_1 U_0$. When it reaches the second mirror, its phase is shifted by $\phi/2 = (2\pi n/\lambda)d$, thus obtaining $U_{02} = e^{i\phi/2} U_{01}$. Part of it is transmitted through the second mirror $U_{T0} = t_2 U_{02} = e^{i\phi/2} t_1 t_2 U_0$. The reflected part obtains the phase shift by π, thus giving $U_{03} = -r_2 U_{02}$. Further, we find that $U_{04} = e^{i\phi/2} U_{03}$, $U_{11} = -r_1 U_{04}$, $U_{12} = e^{i\phi/2} U_{11}$, and $U_{T1} = t_2 U_{12} = e^{i3\phi/2} r_1 r_2 t_1 t_2 U_0$. Additional steps show that $U_{T2} = t_2 U_{22} = e^{i5\phi/2} r_1^2 r_2^2 t_1^2 t_2^2 U_0$. Thus, the summary field amplitude transmitted through the system becomes

$$\begin{aligned} U_T &= U_{T0} + U_{T1} + U_{T2} + \cdots \\ &= U_0 t_1 t_2 e^{i\phi/2} \left(1 + e^{i\phi} r_1 r_2 + \left(e^{i\phi} r_1 r_2\right)^2 + \cdots\right) \quad (92) \\ &= U_0 \frac{t_1 t_2 e^{i\phi/2}}{1 - e^{i\phi} r_1 r_2} = U_0 \frac{\sqrt{1 - r_1^2}\sqrt{1 - r_2^2}\, e^{i\phi/2}}{1 - e^{i\phi} r_1 r_2}. \quad (93) \end{aligned}$$

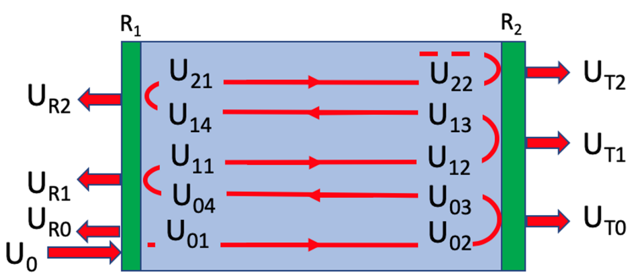

Fig. 3. Schematics of light field propagation in a Fabry–Perot resonator. The light propagates along one horizontal axis. Only for visualization purposes, rays are separated vertically.

When comparing these equations with Eq. (35), we find that $h = r_1 r_2 e^{i\phi} = r_1 r_2 e^{i2\pi nd/\lambda}$ and $|h| = r_1 r_2$, with the exception that the correction of the first amplitude is needed to become $U_0 t_1 t_2 e^{i\phi/2}$.

An alternative way [35] to obtain Eq. (93) is as follows. We use the summary amplitudes of fields propagating outside and inside the resonator: incident field amplitude U_0, reflected field amplitude U_R, transmitted field amplitude U_T, field amplitude in the resonator close to left mirror propagating in the right direction U_1, and the field amplitude in the resonator close to left mirror propagating in the left direction U_4. They have relations $U_1 = t_1 U_0 - r_1 U_4$, $U_R = t_1 U_4 + r_1 U_0$, $U_4 = -U_1 r_2 e^{i\phi}$, and $U_T = U_1 t_2 e^{i\phi/2}$ from which U_T can be derived. This alternative provides a fast way to obtain the final equation but lacks the clarity of its relation to the interference phenomena that is highlighted in this paper.

Equation (93) can be transformed using operations similar to those used for Eqs. (36) and (37); then, we obtain the transmitted field intensity of the Fabry–Perot resonator [36]:

$$I_T = \frac{I_0(1 - r_1^2)(1 - r_2^2)}{(1 - r_1 r_2)^2 + 4 r_1 r_2 \sin^2(\phi/2)}. \tag{94}$$

This can be rewritten as

$$I_T = \frac{I_{T\max}}{1 + (2\mathcal{F}_T/\pi)^2 \sin^2(\phi/2)}, \tag{95}$$

with

$$I_{T\max} = I_0 \frac{(1 - r_1^2)(1 - r_2^2)}{(1 - r_1 r_2)^2}, \tag{96}$$

$$\mathcal{F}_T = \frac{\pi\sqrt{r_1 r_2}}{1 - r_1 r_2}, \tag{97}$$

where $I_{T\max}$ is the maximal transmitted intensity and $\mathcal{F}_T$ is the finesse of the transmitted signal.

Minimal value $I_{T\min}$ of the transmitted intensity in Eq. (94) is obtained when $\sin(\phi/2) = 1$:

$$I_{T\min} = I_0 \frac{(1 - r_1^2)(1 - r_2^2)}{(1 + r_1 r_2)^2} = \frac{I_{T\max}}{1 + (2\mathcal{F}_T/\pi)^2}. \tag{98}$$

Depth of the resonance intensity is

$$\begin{aligned} I_{T\mathrm{res}} &= I_{T\max} - I_{T\min} \quad (99) \\ &= I_0 \frac{4(1 - r_1^2)(1 - r_2^2) r_1 r_2}{(1 - r_1^2 r_2^2)^2} \quad (100) \\ &= K_{T1} I_{T\max} = K_{T2} I_0, \quad (101) \end{aligned}$$

with coefficients

$$K_{T1} = \frac{1}{(\pi/(2\mathcal{F}_T))^2 + 1} = \frac{4 r_1 r_2}{(1 + r_1 r_2)^2}, \tag{102}$$

$$K_{T2} = \frac{4(1 - r_1^2)(1 - r_2^2) r_1 r_2}{(1 - r_1^2 r_2^2)^2}. \tag{103}$$

According to Eq. (31), the signal width of transmitted intensity becomes

$$\Delta\nu_T = \frac{c}{2nd\mathcal{F}_T} = \frac{c}{2\pi nd}\frac{1-r_1r_2}{\sqrt{r_1r_2}}, \tag{104}$$

and the Q-factor is

$$Q_T = \frac{2\pi nd\nu}{c}\frac{\sqrt{r_1r_2}}{1-r_1r_2}. \tag{105}$$

If both mirrors are equal, $r_1 = r_2 = r = \sqrt{R}$; then,

$$I_T = \frac{I_0(1-r^2)^2}{(1-r^2)^2 + 4r^2\sin^2\left(\frac{2\pi dn}{\lambda}\right)} \tag{106}$$

$$= \frac{I_0(1-R)^2}{(1-R)^2 + 4R\sin^2\left(\frac{2\pi dn}{\lambda}\right)}, \tag{107}$$

$$I_{T\max} = I_0, \tag{108}$$

$$I_{T\min} = I_0\frac{(1-r^2)^2}{(1+r^2)^2} = I_0\frac{(1-R)^2}{(1+R)^2}, \tag{109}$$

$$I_{T\text{res}} = I_0\frac{4r^2}{(1+r^2)^2} = I_0\frac{4R}{(1+R)^2}, \tag{110}$$

$$\Delta\nu_T = \frac{c}{2\pi dn}\frac{1-r^2}{r} = \frac{c}{2\pi dn}\frac{1-R}{\sqrt{R}}, \tag{111}$$

$$Q_T = \frac{2\pi dn\nu}{c}\frac{r}{1-r^2} = \frac{2\pi dn\nu}{c}\frac{\sqrt{R}}{1-R}, \tag{112}$$

$$\mathcal{F}_T = \frac{\pi r}{1-r^2} = \frac{\pi\sqrt{R}}{1-R}, \tag{113}$$

$$K_{T1} = K_{T2} = \frac{4r^2}{(1+r^2)^2} = \frac{4R}{(1+R)^2}. \tag{114}$$

Equation (107) looks similar to Eq. (47) with the exception that the intensity has a multiplicator $(1-R)^2$.

To obtain the sharp lines of the Fabry–Perot resonator, reflection coefficient R has to be close to 1. In this case,

$$\Delta\nu_T \approx \frac{c}{2\pi dn}(1-R), \tag{115}$$

$$Q_T \approx \frac{2\pi nd\nu}{c}\frac{1}{1-R}, \tag{116}$$

$$K_{T1} = K_{T2} \approx 1. \tag{117}$$

We can analyze a reflected light of the Fabry–Perot resonator. The reflection from the first mirror gives $U_{R0} = r_1U_0$ (see Fig. 3). Further signals are $U_{R1} = t_1U_{04} = -t_1^2r_2e^{i\phi}U_0$, $U_{R2} = t_1U_{14} = -t_1^2r_2^2r_1e^{i2\phi}U_0 = U_{R1}r_1r_2e^{i\phi}$. Thus,

$$\begin{aligned} U_R &= U_{R0} + U_{R1} + U_{R2} + \cdots \\ &= U_0\left(r_1 - t_1^2r_2e^{i\phi}\left(1 + e^{i\phi}r_1r_2 + \left(e^{i\phi}r_1r_2\right)^2 + \cdots\right)\right) \\ &= U_0\left(r_1 - \frac{t_1^2r_2e^{i\phi}}{1-e^{i\phi}r_1r_2}\right) \\ &= U_0\frac{r_1 - r_2e^{i\phi}}{1-e^{i\phi}r_1r_2}. \end{aligned} \tag{118}$$

For reflected intensity, we obtain

$$I_R = I_0\frac{(r_1-r_2)^2 + 4r_1r_2\sin^2(\phi/2)}{(1-r_1r_2)^2 + 4r_1r_2\sin^2(\phi/2)}. \tag{119}$$

The resonance character of this equation can be seen after mathematical manipulations:

$$I_R = I_0\left(1 - \frac{(1-r_1^2)(1-r_2^2)}{(1-r_1r_2)^2 + 4r_1r_2\sin^2(\phi/2)}\right). \tag{120}$$

We can find that

$$I_0 = I_T + I_R \tag{121}$$

as expected.

As in Eq. (120), phase dependence comes from the denominator, which is equivalent to the intensity of transmitted light in Eq. (94); the finesse of reflected light $\mathcal{F}_R$ is the same as the finesse of transmitted light in Eq. (97):

$$\mathcal{F}_R = \mathcal{F}_T. \tag{122}$$

The maximal value $I_{R\max}$, minimal value $I_{R\min}$, and resonance depth $I_{R\text{res}}$ of reflected intensity I_R are the following:

$$I_{R\max} = I_0\frac{(r_1+r_2)^2}{(1+r_1r_2)^2}, \tag{123}$$

$$I_{R\min} = I_0\frac{(r_1-r_2)^2}{(1-r_1r_2)^2}, \tag{124}$$

$$I_{R\text{res}} = I_{R\max} - I_{R\min}, \tag{125}$$

$$I_{R\text{res}} = I_0\frac{4(1-r_1^2)(1-r_2^2)r_1r_2}{(1-r_1^2r_2^2)^2}, \tag{126}$$

$$= I_{T\text{res}} = K_{R1}I_{R\max} = K_{R2}I_0. \tag{127}$$

Resonance depth coefficients of the reflected light are

$$K_{R1} = \frac{4(1-r_1^2)(1-r_2^2)r_1r_2}{(1-r_1r_2)^2(r_1+r_2)^2} \tag{128}$$

$$= 1 - \frac{(1+r_1r_2)^2(r_1-r_2)^2}{(1-r_1r_2)^2(r_1+r_2)^2}, \tag{129}$$

$$K_{R2} = \frac{4(1-r_1^2)(1-r_2^2)r_1r_2}{(1-r_1^2r_2^2)^2} = K_{T2}. \tag{130}$$

If both mirrors are equal ($r_1 = r_2 = r = \sqrt{R}$), then

$$I_R = I_0\left(1 - \frac{(1-r^2)^2}{(1-r^2)^2 + 4r^2\sin^2(\phi/2)}\right) \tag{131}$$

$$= I_0\left(1 - \frac{(1-R)^2}{(1-R)^2 + 4R\sin^2(\phi/2)}\right) \tag{132}$$

$$I_{R\,\mathrm{max}} = I_0\frac{4r^2}{(1+r^2)^2} = I_0\frac{4R}{(1+R)^2}, \tag{133}$$

$$I_{R\,\mathrm{min}} = 0, \tag{134}$$

$$I_{R\mathrm{res}} = I_0\frac{4r^2}{(1+r^2)^2} = I_0\frac{4R}{(1+R)^2} = I_{T\mathrm{res}}, \tag{135}$$

$$K_{R1} = 1, \tag{136}$$

$$K_{R2} = \frac{4r^2}{(1+r^2)^2} = \frac{4R}{(1+R)^2} = K_{T2}. \tag{137}$$

By inserting equation for ϕ, we obtain

$$I_R = I_0\left(1 - \frac{(1-R)^2}{(1-R)^2 + 4R\sin^2(2\pi dn/\lambda)}\right). \tag{138}$$

Type 2 of the Fabry–Perot resonator [Fig. 1(b)] can be analyzed as well. We assume that the resonator is filled with media with refractive index n, which is still smaller than the refractive index of plain parallel surfaces of both sides of the resonator. A similar ray scheme as in Fig. 3 can be used. Here, an additional index "B" will be used to describe each amplitude. For example, U_{B01} will be used as a substitution of U_{01} in Fig. 3, which is used for the Type 1 Fabry–Perot resonator. It can be found that $U_{B01} = U_{01}$, $U_{B02} = U_{02}$, $U_{B03} = -U_{03}$, $U_{TB0} = U_{T0}$, $U_{B04} = -U_{04}$, $U_{B11} = U_{11}$, $U_{B12} = U_{12}$, $U_{TB1} = U_{T1}$, and $U_{TB2} = U_{T2}$; the summary transmission field U_{FB} is equal to U_F. For reflected beams, $U_{RB0} = -U_{R0}$, $U_{RB1} = -U_{R1}$, $U_{RB2} = -U_{R2}$, and a summary reflected beam $U_{RB} = -U_R$, which has the opposite sign compared with Type 1. Intensity distributions are equal for both types of Fabry–Perot resonators.

B. Circular Resonator Coupled to One Waveguide

Let us explore the situation when a circular whispering gallery mode resonator with radius a is coupled to a waveguide (Fig. 4). The field in this resonator can be modeled as reflected field U_R of the Fabry–Perot resonator when the second mirror is fully reflective, $R_2 = 1$ and $R_1 = R$. In this case, the absorption and dissipation of the field were not taken into account. Thus, intensity distribution is obtained from Eq. (120) and becomes $I = I_0$, which means that all fields are transmitted through the system.

We will describe a model of a waveguide coupled to a circular resonator, taking into account field decay in the system. This system is called an "optical all-pass filter." Coupling of the waveguide and the resonator will be described by the reflection

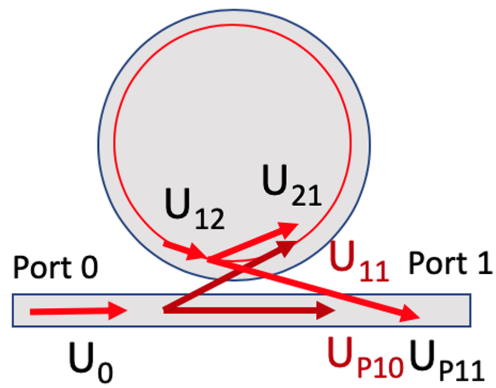

Fig. 4. Light propagation in a circular resonator coupled to a waveguide.

coefficient $r = \sqrt{R}$, transmission coefficient $t = \sqrt{1-r^2}$, one loop light path length in the resonator is L, giving the phase shift per loop $\phi = 2\pi nL/\lambda$, and the field decay rate $e^{-\beta}$ with

$$\beta = t_0/(2\tau) = nL/(2c\tau), \tag{139}$$

where t_0 is the time the light travels one loop in the resonator, τ is a decay rate of a signal in the resonator, n is a refractive index of the resonator, and c is the speed of light.

Let us obtain the summary transmitted light amplitude U_{P1} of the all-pass filter in Port 1 (Fig. 4). The light with amplitude $U_0 = \sqrt{I_0}$ enters the waveguide from the left side. Part of this amplitude $U_{P10} = rU_0$ is passing through the waveguide without entering the resonator. Another part $U_{11} = tU_0$ enters the resonator. After travelling one loop in the resonator, the amplitude of the wave becomes $U_{12} = -e^{i\phi}e^{-\beta}U_{11}$. This field reflects back into the resonator as $U_{21} = -rU_{12}$. Another part is transmitted to the waveguide as amplitude $U_{P11} = tU_{12} = -e^{i\phi}e^{-\beta}t^2U_0$. The field amplitude U_{21} after travelling the next loop in the resonator turns into $U_{22} = -e^{i\phi}e^{-\beta}U_{21}$. This field is transmitted to the waveguide as $U_{P12} = tU_{22} = -e^{i2\phi}e^{-2\beta}rt^2U_0 = U_{P11}\cdot(e^{i\phi}e^{-\beta}r)$ and is reflected into the resonator as $U_{31} = -rU_{22}$. Further, U_{31} after one loop in the resonator turns into $U_{32} = -e^{i\phi}e^{-\beta}U_{31}$. It is transmitted to the waveguide as $U_{P13} = tU_{32} = e^{i\phi}e^{-\beta}rtU_{22} = e^{i\phi}e^{-\beta}rU_{P12} = U_{P11}\cdot(e^{i\phi}e^{-\beta}r)^2$. In a similar manner, the further series of reflected and transmitted signals can be found. Finally, the summary transmitted light amplitude U_{P1} of the all-pass filter in Port 1 is obtained as a sum of series:

$$U_{P1} = U_{P10} + U_{P11} + U_{P12} + \cdots \tag{140}$$

$$= U_0 r - U_0 t^2 e^{i\phi}e^{-\beta} \times \left(1 + e^{i\phi}e^{-\beta}r + \left(e^{i\phi}e^{-\beta}r\right)^2 + \cdots\right) \tag{141}$$

$$= U_0\left(r - \frac{(1-r^2)e^{i\phi}e^{-\beta}}{1 - e^{i\phi}e^{-\beta}r}\right) \tag{142}$$

$$= U_0\left(\frac{r - e^{i\phi}e^{-\beta}}{1 - re^{i\phi}e^{-\beta}}\right). \tag{143}$$

An alternative approach [37–39] obtains Eq. (143) using summary field amplitudes in a waveguide and resonator. Now, the incident field amplitude is taken to be U_0, summary transmitted field amplitude U_P, and field amplitudes U_1 and U_2 in the resonator before and after the connection point with the waveguide, respectively. They hold relations $U_P = rU_0 + itU_1$, $U_2 = itU_0 + rU_1$, and $U_1 = U_2 e^{i\phi} e^{-\beta}$ from which U_P can be derived. This alternative provides a fast way to obtain the final equation but lacks the clarity of its relation to the interference phenomena that are highlighted in this paper.

The transmitted field intensity in Port 1 is

$$I_{P1} = |U_{P1}|^2 = I_0 \frac{\left(r - e^{-\beta}\right)^2 + 4re^{-\beta}\sin^2(\phi/2)}{(1 - re^{-\beta})^2 + 4re^{-\beta}\sin^2(\phi/2)} \tag{144}$$

$$= I_0 \left(1 - \frac{(1 - r^2)\left(1 - e^{-2\beta}\right)}{(1 - re^{-\beta})^2 + 4re^{-\beta}\sin^2(\phi/2)}\right). \tag{145}$$

It can be rewritten as

$$I_{P1} = I_0 - \frac{I_{P11\,\max}}{1 + (2\mathcal{F}_{P1}/\pi)^2 \sin^2(\phi/2)}, \tag{146}$$

$$I_{P11\,\max} = I_0 \frac{(1 - r^2)\left(1 - e^{-2\beta}\right)}{(1 - re^{-\beta})^2} \tag{147}$$

$$= I_0 \left(1 - \left(\frac{r - e^{-\beta}}{1 - re^{-\beta}}\right)^2\right), \tag{148}$$

$$\mathcal{F}_{P1} = \frac{\pi\sqrt{r}e^{-\beta/2}}{1 - re^{-\beta}}, \tag{149}$$

where $\mathcal{F}_{P1}$ is the finesse of the all-pass filter signal. According to Eq. (32), the Q-factor of this signal is

$$Q_{P1} = \frac{\pi n L \nu}{c} \frac{\sqrt{r}e^{-\beta/2}}{1 - re^{-\beta}}. \tag{150}$$

The minimal value $I_{P1\,\min}$ of the intensity I_{P1} in Eq. (146) is obtained when $\sin(\phi/2) = 0$:

$$I_{P1\,\min} = I_0 \left(\frac{r - e^{-\beta}}{1 - re^{-\beta}}\right)^2. \tag{151}$$

Alternatively, this condition corresponds to the largest intensity accumulated in the resonator ring [40].

The maximal value $I_{P1\,\max}$ of the intensity I_{P1} in Eq. (146) is obtained when $\sin^2(\phi/2) = 1$:

$$I_{P1\,\max} = I_0 \left(\frac{r + e^{-\beta}}{1 + re^{-\beta}}\right)^2. \tag{152}$$

The resonance depth $I_{P1\mathrm{res}}$ of the transmitted intensity I_{P1} is

$$I_{P1\mathrm{res}} = I_{\max} - I_{\min} \tag{153}$$

$$= I_0 \frac{4re^{-\beta}(1 - r^2)\left(1 - e^{-2\beta}\right)}{\left(1 - r^2 e^{-2\beta}\right)^2} \tag{154}$$

$$= K_{1P1} I_{P1\,\max} = K_{2P1} I_0, \tag{155}$$

$$K_{1P1} = \frac{4re^{-\beta}(1 - r^2)\left(1 - e^{-2\beta}\right)}{(1 - re^{-\beta})^2 (r + e^{-\beta})^2}, \tag{156}$$

$$K_{2P1} = \frac{4re^{-\beta}(1 - r^2)\left(1 - e^{-2\beta}\right)}{\left(1 - r^2 e^{-2\beta}\right)^2}. \tag{157}$$

According to Eq. (31), the signal width of transmitted intensity becomes

$$\Delta\nu_{P1} = \frac{c}{\pi n L} \frac{1 - re^{-\beta}}{\sqrt{r}e^{-\beta/2}}. \tag{158}$$

If there is a slow decay, $(\beta \to 0)$ and $r \nrightarrow 1$, then the resonance depth in Eq. (154) becomes

$$I_{P1\mathrm{res}} \approx I_0 \frac{8r}{1 - r^2}\beta. \tag{159}$$

If there is no decay ($\beta = 0$), then the resonance depth is 0, which means that no resonance can be detected by intensity measurements. This is an important conclusion, despite the fact that, in this situation, the Q-factor has some value as derived from Eq. (150):

$$Q_{P10} = \frac{\pi n L \nu}{c} \frac{\sqrt{r}}{1 - r}. \tag{160}$$

Let us analyze the Q-factor in Eq. (150):

$$\frac{1}{Q_{P1}} = \frac{c}{\pi n L \nu} \frac{1 - re^{-\beta}}{\sqrt{r}e^{-\beta/2}} \tag{161}$$

$$= \frac{c}{\pi n L \nu \sqrt{r}} \left(e^{\beta/2} - re^{-\beta/2}\right). \tag{162}$$

Let us assume that decay is slow ($\beta \approx 0$), expand Eq. (162) in Taylor series around the value of $\beta = 0$, take the first two elements of the series and use the definition in Eq. (139):

$$\frac{1}{Q_{P1}} \approx \frac{c}{\pi n L \nu \sqrt{r}}(1 - r) + \frac{c}{2\pi n L \nu \sqrt{r}}(1 + r)\beta \tag{163}$$

$$= \frac{1}{Q_{P10}} + \frac{c}{2\pi n L \nu}\beta \frac{1 + r}{\sqrt{r}} \tag{164}$$

$$= \frac{1}{Q_{P10}} + \frac{c}{4\pi \nu \tau} \frac{1 + r}{\sqrt{r}}. \tag{165}$$

For Q_{P10} to take the largest value, r has to be close to 1. Therefore, now we can expand the second term in Eq. (165) in Taylor series, respectively, to r and around its value 1 and take first two elements. We obtain

$$\frac{c}{4\pi\nu\tau} \frac{1 + r}{\sqrt{r}} = \frac{c}{4\pi\nu\tau}\left(r^{-1/2} + \sqrt{r}\right) \approx \frac{c}{2\pi\nu\tau} \tag{166}$$

$$= \frac{1}{Q_{P1\tau}}, \tag{167}$$

where the decay is described as $Q_{P1\tau}$—factor, according to Eqs. (23) and (25).

Now the Q-factor of the optical all-pass filter can be described as

$$\frac{1}{Q_{P1}} \approx \frac{1}{Q_{P10}} + \frac{1}{Q_{P1\tau}}. \tag{168}$$

Here, we see that Q-factors of various processes in the system are inversely summarized according to the rule of Eq. (29).

C. Circular Resonator Coupled to Two Waveguides

A circular resonator with two waveguides can be analyzed (see Fig. 5). Such a resonator is called an "add-drop filter." It can be modeled as a Fabry–Perot resonator with various reflection coefficients of mirrors. The decay of signal in the system can be described in similarity with the description of the all-pass filter. By comparing Eq. (118) when $r_2 = 1$ and $r_1 = r$ with Eq. (143), we see that decay could be introduced by substituting $e^{i\phi}$ with $e^{i\phi}e^{-\beta}$ in Eq. (118). This is logical, as a phase shift ϕ was obtained by light travelling one loop in the resonator; in this path, the decay $e^{-\beta}$ was obtained. Now transmitted light field amplitude U_{P1} through Port 1 can be expressed from Eq. (118) by substituting $e^{i\phi}$ with $e^{i\phi}e^{-\beta}$:

$$U_{P1} = U_0 \frac{r_1 - r_2 e^{i\phi} e^{-\beta}}{1 - r_1 r_2 e^{i\phi} e^{-\beta}}. \tag{169}$$

Equation (169) can also be obtained from Eq. (118) if r_2 is substituted by $r_2 e^{-\beta}$. Taking this into account, we can write the intensity of Port 1 as Eq. (120), with r_2 substituted by $r_2 e^{-\beta}$ and R_2 substituted by $R_2 e^{-\beta/2}$, or as Eq. (145) with $e^{-\beta}$ substituted by $r_2 e^{-\beta}$ and r substituted by r_1:

$$\begin{aligned} I_{P1} &= |U_{P1}|^2 \\ &= I_0 \left(1 - \frac{(1 - r_1^2)\left(1 - r_2^2 e^{-2\beta}\right)}{\left(1 - r_1 r_2 e^{-\beta}\right)^2 + 4 r_1 r_2 e^{-\beta} \sin^2(\phi/2)} \right). \end{aligned} \tag{170}$$

It can be rewritten as

$$I_{P1} = I_0 - \frac{I_{P11\,\max}}{1 + (2\mathcal{F}_T/\pi)^2 \sin^2(\phi/2)}, \tag{171}$$

$$I_{P11\,\max} = I_0 \frac{(1 - r_1^2)\left(1 - r_2^2 e^{-2\beta}\right)}{\left(1 - r_1 r_2 e^{-\beta}\right)^2}, \tag{172}$$

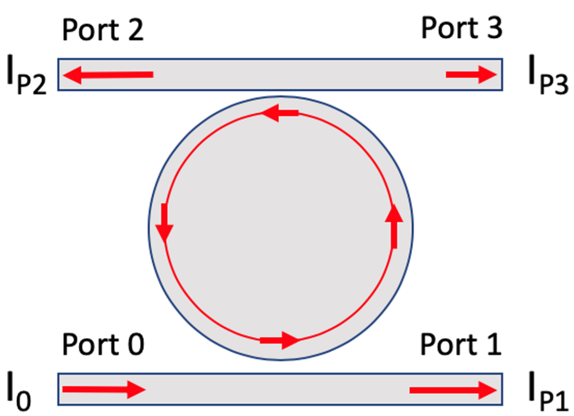

Fig. 5. Light propagation in circular resonator coupled to two waveguides.

$$\mathcal{F}_{P1} = \frac{\pi \sqrt{r_1 r_2 e^{-\beta/2}}}{1 - r_1 r_2 e^{-\beta}}, \tag{173}$$

where $\mathcal{F}_{P1}$ is the finesse of the add-drop filter signal in Port 1. According to Eq. (32), the Q-factor of this signal in Port 1 is

$$Q_{P1} = \frac{\pi n L \nu}{c} \frac{\sqrt{r_1 r_2 e^{-\beta/2}}}{1 - r_2 r_2 e^{-\beta}}. \tag{174}$$

The minimal value $I_{P1\,\min}$ of I_{P1} is obtained when $\sin(\phi/2) = 0$:

$$I_{P1\,\min} = I_0 \left(\frac{r_1 - r_2 e^{-\beta}}{1 - r_1 r_2 e^{-\beta}} \right)^2. \tag{175}$$

The maximal value $I_{P1\,\max}$ of I_{P1} is obtained when $\sin^2(\phi/2) = 1$:

$$I_{P1\,\max} = I_0 \left(\frac{r_1 + r_2 e^{-\beta}}{1 + r_1 r_2 e^{-\beta}} \right)^2. \tag{176}$$

The resonance depth is

$$I_{P1\mathrm{res}} = I_{P1\,\max} - I_{P1\,\min} \tag{177}$$

$$= I_0 \frac{4 r_1 r_2 e^{-\beta} (1 - r_1^2) \left(1 - r_2^2 e^{-2\beta}\right)}{\left(1 - r_1^2 r_2^2 e^{-2\beta}\right)^2} \tag{178}$$

$$= K_{1P1} I_{P1\,\max} = K_{2P1} I_0, \tag{179}$$

$$K_{1P1} = \frac{4 r_1 r_2 e^{-\beta} (1 - r_1^2) \left(1 - r_2^2 e^{-2\beta}\right)}{\left(1 - r_1 r_2 e^{-\beta}\right)^2 \left(r_1 + r_2 e^{-\beta}\right)^2}, \tag{180}$$

$$K_{2P1} = \frac{4 r_1 r_2 e^{-\beta} (1 - r_1^2) \left(1 - r_2^2 e^{-2\beta}\right)}{\left(1 - r_1^2 r_2^2 e^{-2\beta}\right)^2}. \tag{181}$$

If there is a slow decay, $(\beta \to 0)$ and r_1, $r_2 \nrightarrow 1$, then the resonance depth in Eq. (178) becomes

$$I_{\mathrm{res}} \approx I_0 \frac{4 r_1 r_2 (1 - r_1^2)(1 - r_2^2)}{(1 - r_1^2 r_2^2)^2}. \tag{182}$$

In Port 2 (see Fig. 5), the output signal amplitude U_{P2} can be obtained from Eq. (93) taking into account that $e^{i\phi}$ has to be substituted by $e^{i\phi}e^{-\beta}$:

$$U_{P2} = U_0 \frac{\sqrt{1 - r_1^2}\sqrt{1 - r_2^2}\, e^{i\phi/2} e^{-\beta/2}}{1 - r_1 r_2 e^{i\phi} e^{-\beta}}. \tag{183}$$

The corresponding field intensity $I_{P2} = |U_{P2}|^2$ in Port 2 becomes

$$I_{P2} = I_0 \frac{(1 - r_1^2)(1 - r_2^2) e^{-\beta}}{\left(1 - r_1 r_2 e^{-\beta}\right)^2 + 4 r_1 r_2 e^{-\beta} \sin^2(\phi/2)} \tag{184}$$

$$= \frac{I_{P2\,\max}}{1 + (2\mathcal{F}_{P2}/\pi)^2 \sin^2(\phi/2)}, \tag{185}$$

where maximal value $I_{P2\,\max}$ and the finesse $\mathcal{F}_{P2}$ can be derived as

$$I_{P2\,\max} = \frac{I_0(1-r_1^2)(1-r_2^2)e^{-\beta}}{\left(1-r_1r_2e^{-\beta}\right)^2}, \tag{186}$$

$$\mathcal{F}_{P2} = \frac{\pi\sqrt{r_1r_2}e^{-\beta/2}}{1-r_1r_2e^{-\beta}} = \mathcal{F}_{P1}. \tag{187}$$

The corresponding Q-factor of the signal in Port 2 is

$$Q_{P2} = Q_{P1} = \frac{\pi nL\nu}{c}\frac{\sqrt{r_1r_2}e^{-\beta/2}}{1-r_2r_2e^{-\beta}}. \tag{188}$$

The minimal value $I_{P2\,\min}$ of the intensity I_{P2} in Eq. (184) is obtained when $\sin(\phi/2) = 1$:

$$I_{P2\,\min} = \frac{I_0(1-r_1^2)(1-r_2^2)e^{-\beta}}{\left(1+r_1r_2e^{-\beta}\right)^2} \tag{189}$$

$$= \frac{I_{P2\,\max}}{1+(2\mathcal{F}_{P2}/\pi)^2}. \tag{190}$$

The resonance depth $I_{P2\text{res}}$ of the intensity I_{P2} becomes

$$I_{P2\text{res}} = I_{P2\,\max} - I_{P2\,\min} \tag{191}$$

$$= I_0\frac{4(1-r_1^2)(1-r_2^2)r_1r_2e^{-2\beta}}{\left(1-r_1^2r_2^2e^{-2\beta}\right)^2} \tag{192}$$

$$= K_{1P2}I_{P2\,\max} = K_{2P2}I_0, \tag{193}$$

with corresponding coefficients

$$K_{1P2} = \frac{1}{(\pi/(2\mathcal{F}_{P2}))^2+1} = \frac{4r_1r_2e^{-\beta}}{\left(1+r_1r_2e^{-\beta}\right)^2}, \tag{194}$$

$$K_{2P2} = \frac{4(1-r_1^2)(1-r_2^2)r_1r_2e^{-2\beta}}{\left(1-r_1^2r_2^2e^{-2\beta}\right)^2}. \tag{195}$$

Table 1. Summary of Main Equations That Describe Parameters of Resonances

	Q-factor	
$Q = 2\pi\frac{\text{storedenergy}}{\text{energy loss per oscillation period}}$	$Q = 2\pi\nu\tau = \tau\omega = \frac{2\pi\tau c}{\lambda} = \frac{\omega}{\Delta\omega} = \frac{\nu}{\Delta\nu} = \frac{\lambda}{\Delta\lambda}$	$Q = \mathcal{F}\frac{nL\nu}{c} = \mathcal{F}\frac{L}{(\lambda/n)} = \mathcal{F}m$
	Interference of an infinite number of waves of progressively smaller amplitudes and equal phase difference	
$U_1 = \sqrt{I_0},\ U_2 = hU_1,\ U_3 = hU_2 = h^2U_1, \ldots$ $h = \vert h\vert e^{i\phi}, \vert h\vert < 1$ $U = U_1+U_2+U_3+\ldots$ $I = \vert U\vert^2 = \frac{I_0}{(1-\vert h\vert)^2+4\vert h\vert\sin^2(\phi/2)}$ $I_{\max} = \frac{I_0}{(1-\vert h\vert)^2}$ $I_{\min} = \frac{I_0}{(1+\vert h\vert)^2}$ $I_{\text{res}} = I_{\max} - I_{\min} = \frac{4\vert h\vert I_0}{(1-\vert h\vert^2)^2}$	$I_{\text{res}} = K_1\cdot I_{\max} = K_2\cdot I_0$ $K_1 = \frac{4\vert h\vert}{(1+\vert h\vert)^2}$ $K_2 = \frac{4\vert h\vert}{(1-\vert h\vert^2)^2}$ $\Delta\phi(\text{FWHM}) = 4\arcsin\frac{1-\vert h\vert}{2\sqrt{\vert h\vert}}$ for slow decay ($\vert h\vert \approx 1$) $\Delta\phi(\text{FWHM}) \approx 2\frac{1-\vert h\vert}{\sqrt{\vert h\vert}}$ $\mathcal{F} \approx \frac{\pi\sqrt{\vert h\vert}}{1-\vert h\vert} \approx \frac{\pi}{1-\vert h\vert}$	$Q \approx \frac{\pi nL\nu}{c}\frac{1}{1-\vert h\vert}$ $K_1 \approx 1-(\pi/(2\mathcal{F}))^2 \approx 1$ $K_2 \approx (\mathcal{F}/\pi)^2$ close to resonances $\phi-\phi_{\text{res}} \approx 0$ and $I \approx \frac{I_{\max}}{1+(\mathcal{F}/\pi)^2(\phi-\phi_{\text{res}})^2}$
	Intensity distribution of WGMR for slow decay ($\vert h\vert \approx 1$)	
$\phi = k\cdot L = \frac{2\pi n}{\lambda}\cdot L = \frac{2\pi nL}{c}\cdot\nu$ $\vert h\vert = e^{-\beta} = e^{-t_0/(2\tau)} = e^{-nL/(2c\tau)}$ $= e^{-\pi nL\nu/(cQ)} \approx 1-\pi nL\nu/(cQ)$	$I = \frac{I_0}{\left(1-e^{-\frac{\pi nL\nu}{cQ}}\right)^2+4e^{-\frac{\pi nL\nu}{cQ}}\sin^2(\frac{\pi nL}{c}\nu)}$ $\approx \frac{I_0}{(\frac{\pi nL\nu}{cQ})^2+4\sin^2(\frac{\pi nL}{c}\nu)}$ $\Delta\nu \approx \frac{c}{\pi nL}\frac{1-\vert h\vert}{\sqrt{\vert h\vert}} \approx \frac{1}{2\pi\tau}$	$\Delta\lambda \approx \frac{\lambda^2}{\pi nL}\frac{1-\vert h\vert}{\sqrt{\vert h\vert}} \approx \frac{\lambda^2}{2\pi c\tau}$ $Q \approx \frac{\pi nL\nu}{c}\frac{\sqrt{\vert h\vert}}{1-\vert h\vert} \approx 2\pi\nu\tau$ $\mathcal{F} \approx \frac{\pi\sqrt{\vert h\vert}}{1-\vert h\vert} \approx \frac{\pi}{1-\vert h\vert} \approx \frac{2\pi c\tau}{nL}$
	Fabry–Perot resonances	
$U_1 = U_{T0} = \sqrt{I_0(1-r_1^2)(1-r_2^2)}e^{i\phi/2}$ $h = r_1r_2e^{i\phi}$ $\phi = 4\pi nd/\lambda$ $\vert h\vert = r_1r_2$	Transmitted signal $I_T = \frac{I_{T\,\max}}{1+(2\mathcal{F}_T/\pi)^2\sin^2(\phi/2)}$ $\mathcal{F}_T = \frac{\pi\sqrt{r_1r_2}}{1-r_1r_2}$ $I_{T\,\max} = I_0\frac{(1-r_1^2)(1-r_2^2)}{(1-r_1r_2)^2}$ $I_{T\,\min} = I_0\frac{(1-r_1^2)(1-r_2^2)}{(1+r_1r_2)^2}$	$\Delta\nu_T = \frac{c}{2nd\mathcal{F}_T} = \frac{c}{2\pi nd}\frac{1-r_1r_2}{\sqrt{r_1r_2}}$ $Q_T = \frac{2\pi nd\nu}{c}\frac{\sqrt{r_1r_2}}{1-r_1r_2}$ Reflected signal $I_R = I_0 - I_T$
	Circular resonator coupled to one waveguide	
$h = re^{-\beta}e^{i\phi}$ $\phi = 2\pi nL/\lambda$ $\vert h\vert = re^{-\beta}$ $\beta = t_0/(2\tau) = nL/(2c\tau)$	$I_{P1} = I_0 - \frac{I_{P11\,\max}}{1+(2\mathcal{F}_{P1}/\pi)^2\sin^2(\phi/2)}$ $\mathcal{F}_{P1} = \frac{\pi\sqrt{r}e^{-\beta/2}}{1-re^{-\beta}}$ $I_{P11\,\max} = I_0\frac{(1-r^2)(1-e^{-2\beta})}{(1-re^{-\beta})^2}$ $I_{P1\,\max} = I_0(\frac{r+e^{-\beta}}{1+re^{-\beta}})^2$	$I_{P1\,\min} = I_0(\frac{r-e^{-\beta}}{1-re^{-\beta}})^2$ $\Delta\nu_{P1} = \frac{c}{\pi nL}\frac{1-re^{-\beta}}{\sqrt{r}e^{-\beta/2}}$ $Q_{P1} = \frac{\pi nL\nu}{c}\frac{\sqrt{r}e^{-\beta/2}}{1-re^{-\beta}}$
	Circular resonator coupled to two waveguides	
$I_{P1} = I_0 - \frac{I_{P11\,\max}}{1+(2\mathcal{F}_{P1}/\pi)^2\sin^2(\phi/2)}$ $I_{P11\,\max} = I_0\frac{(1-r_1^2)(1-r_2^2e^{-2\beta})}{(1-r_1r_2e^{-\beta})^2}$	$\mathcal{F}_{P1} = \frac{\pi\sqrt{r_1r_2}e^{-\beta/2}}{1-r_1r_2e^{-\beta}}$ $Q_{P1} = \frac{\pi nL\nu}{c}\frac{\sqrt{r_1r_2}e^{-\beta/2}}{1-r_2r_2e^{-\beta}}$	$I_{P1\,\max} = I_0(\frac{r_1+r_2e^{-\beta}}{1+r_1r_2e^{-\beta}})^2$ $I_{P1\,\min} = I_0(\frac{r_1-r_2e^{-\beta}}{1-r_1r_2e^{-\beta}})^2$

Within our model, the light intensity in Port 3 is $I_{P3} = 0$, as no light travels in the opposite direction to the incident light.

The dissipated intensity I_D of the add-drop filter can be obtained as

$$I_D = I_0 - (I_{P1} + I_{P2}) \tag{196}$$

$$= I_0 \frac{(1 - r_1^2)\left(1 + r_2^2 e^{-\beta}\right)\left(1 - e^{-\beta}\right)}{\left(1 - r_1 r_2 e^{-\beta}\right)^2 + 4 r_1 r_2 e^{-\beta} \sin^2(\phi/2)}. \tag{197}$$

When there is no decay, $(\beta = 0)$, the dissipated field vanishes $I_D = 0$, as expected from Eq. (121).

When the coupling of the resonator to both waveguides is equal, which means $r_1 = r_2 = r$, then the characteristic parameters of the field in Port 1 become

$$I_{P1} = I_0 \left(1 - \frac{(1 - r^2)\left(1 - r^2 e^{-2\beta}\right)}{\left(1 - r^2 e^{-\beta}\right)^2 + 4 r^2 e^{-\beta} \sin^2(\phi/2)}\right), \tag{198}$$

$$\mathcal{F}_{P1} = \frac{\pi r e^{-\beta/2}}{1 - r^2 e^{-\beta}}, \tag{199}$$

$$Q_{P1} = \frac{\pi n L \nu}{c} \frac{r e^{-\beta/2}}{1 - r^2 e^{-\beta}}. \tag{200}$$

4. CONCLUSION

Main derived formulas as a result of this paper are summarized in Table 1. They are ordered in a way that asserts the similarity of Fabry–Perot and whispering gallery mode resonances with those of an interference of an infinite number of waves of progressively smaller amplitudes and equal phase differences.

We presented the classical analytical description of resonances in Fabry–Perot and whispering gallery mode resonators. Basic terms such as wavelength in media, resonance condition for wavelength and frequency, including an integral form of resonance condition in case of nonhomogenous media, free spectral range, Q-factor, summation principle of Q-factors of various processes, and finesse were introduced. Interference of an infinite number of waves of progressively smaller amplitudes and equal phase differences were described, its intensity distribution, maximal intensity, minimal intensity, resonance depth, resonance condition, resonance width, Q-factor, and finesse were derived. The case of a small decay was analyzed.

Fabry–Perot resonators with nonequal and equal reflection coefficients of their mirrors were described. The amplitudes of fields in a resonator, summary amplitude of transmitted and reflected fields, intensity distribution, maximal and minimal intensities, resonance depth, resonance width, finesse, Q-factor, and corresponding values for slow decay were analyzed.

Circular resonators coupled to one and two waveguides were described. Field decay in the resonator was introduced. Characteristics of resonances were derived and presented in the form that allows them to compare with Fabry–Perot resonances and general case of the interference of an infinite number of waves of progressively smaller amplitudes and equal phase differences.

A description of the resonances provided in this paper is a useful tool for reference when forming an in-depth understanding of optical resonances, analyzing experimental data, and searching for ways to optimize resonator systems.

Summarizing our paper represents a detailed description of the theoretical approach describing features of the resonators for general introduction in the topics of optical resonances.

Funding. Latvijas Zinātnes Padome (lzp-2018/1-0510); Centrālā finanšu un līgumu agentūra (1.1.1.5/19/A/003, 1.1.1.1/16/A/259).

Acknowledgment. The author is thankful to R. A. Ganeev for useful comments on the paper.

Disclosures. The author declares no conflicts of interests.

Data Availability. Data underlying the results presented in this paper are not publicly available at this time but may be obtained from the author upon reasonable request.

REFERENCES

1. S. Yang, Y. Wang, and H. Sun, "Advances and prospects for whispering gallery mode microcavities," Adv. Opt. Mater. **3**, 1136–1162 (2015).
2. K. J. Vahala, "Optical microcavities," Nature **424**, 839–846 (2003).
3. T. J. Kippenberg, R. Holzwarth, and S. A. Diddams, "Microresonator-based optical frequency combs," Science **332**, 555–559 (2011).
4. I. Brice, A. Pirktina, A. Ubele, K. Grundsteins, A. Atvars, R. Viter, and J. Alnis, "Development of optical WGM resonators for biosensors," Proc. SPIE **10592**, 105920B (2017).
5. I. Brice, K. Grundsteins, A. Atvars, J. Alnis, and R. Viter, "Whispering gallery mode resonators coated with Au nanoparticles," Proc. SPIE **11089**, 110891T (2019).
6. A. Chiasera, Y. Dumeige, P. Féron, M. Ferrari, Y. Jestin, G. Conti, S. Pelli, S. Soria, and G. Righini, "Spherical whispering-gallery-mode microresonators," Laser Photon. Rev. **4**, 457–482 (2010).
7. D. K. Armani, T. J. Kippenberg, S. M. Spillane, and K. J. Vahala, "Ultra-high-Q toroid microcavity on a chip," Nature **421**, 925–928 (2003).
8. W. Bogaerts, P. De Heyn, T. Van Vaerenbergh, K. De Vos, S. Kumar Selvaraja, T. Claes, P. Dumon, P. Bienstman, D. Van Thourhout, and R. Baets, "Silicon microring resonators," Laser Photon. Rev. **6**, 47–73 (2012).
9. J. Alnis, A. Schliesser, C. Y. Wang, J. Hofer, T. J. Kippenberg, and T. W. Hänsch, "Thermal-noise-limited crystalline whispering-gallery-mode resonator for laser stabilization," Phys. Rev. A **84**, 011804 (2011).
10. L. Cai, J. Pan, and S. Hu, "Overview of the coupling methods used in whispering gallery mode resonator systems for sensing," Opt. Laser Eng. **127**, 105968 (2020).
11. I. Brice, R. Viter, K. Draguns, K. Grundsteins, A. Atvars, J. Alnis, E. Coy, and I. Iatsunskyi, "Whispering gallery mode resonators covered by ZnO nanolayer," Optik **219**, 165296 (2020).
12. M. L. Gorodetsky, A. A. Savchenkov, and V. S. Ilchenko, "Ultimate Q of optical microsphere resonators," Opt. Lett. **21**, 453–455 (1996).
13. R. Berkis, J. Alnis, A. Atvars, I. Brice, K. Draguns, and K. Grundsteins, "Quality factor measurements for PMMA WGM microsphere resonators using fixed wavelength laser and temperature changes," in *IEEE 9th International Conference Nanomaterials: Applications & Properties (NAP)* (IEEE, 2019), paper 01P05.
14. P. K. Reinis, L. Milgrave, K. Draguns, I. Brice, J. Alnis, and A. Atvars, "High-sensitivity whispering gallery mode humidity sensor based on glycerol microdroplet volumetric expansion," Sensors **21**, 1746 (2021).
15. P. Zijlstra, K. L. van der Molen, and A. P. Mosk, "Spatial refractive index sensor using whispering gallery modes in an optically trapped microsphere," Appl. Phys. Lett. **90**, 161101 (2007).
16. M. R. Foreman, J. D. Swaim, and F. Vollmer, "Whispering gallery mode sensors," Adv. Opt. Photon. **7**, 168–240 (2015).

17. I. Brice, K. Grundsteins, A. Atvars, J. Alnis, R. Viter, and A. Ramanavicius, "Whispering gallery mode resonator and glucose oxidase based glucose biosensor," Sens. Actuators B Chem. **318**, 128004 (2020).
18. M. D. Baaske, M. R. Foreman, and F. Vollmer, "Single-molecule nucleic acid interactions monitored on a label-free microcavity biosensor platform," Nat. Nanotechnol. **9**, 933–939 (2014).
19. D. Braunstein, A. Khazanov, G. Koganov, and R. Shuker, "Lowering of threshold conditions for nonlinear effects in a microsphere," Phys. Rev. A **53**, 3565 (1996).
20. A. L. Gaeta, M. Lipson, and T. J. Kippenberg, "Photonic-chip-based frequency combs," Nat. Photonics **13**, 158–169 (2019).
21. A. N. Oraevsky, "Whispering-gallery waves," Quantum Electron. **32**, 377–400 (2002).
22. E. Franchimon, K. Hiremath, R. Stoffer, and M. Hammer, "Interaction of whispering gallery modes in integrated optical microring or microdisk circuits: Hybrid coupled mode theory model," J. Opt. Soc. Am. B **30**, 1048–1057 (2013).
23. B. Milanović, B. Radjenović, and M. Radmilović-Radjenović, "Three-dimensional finite-element modeling of optical microring resonators," Phys. Scr. **T149**, 014026 (2012).
24. A. Kaplan, T. Tomes, M. Carmon, M. Kozlov, O. Cohen, G. Bartal, and H. G. L. Schwefel, "Finite element simulation of a perturbed axial-symmetric whispering-gallery mode and its use for intensity enhancement with a nanoparticle coupled to a microtoroid," Opt. Express **21**, 14169–14180 (2013).
25. X. Jin, Y.-D. Yang, J.-L. Xiao, and Y.-Z. Huang, "Mode control for microring resonators with inner-wall gratings," J. Opt. Soc. Am. B **33**, 1906–1912 (2016).
26. K. Draguns, I. Brice, A. Atvars, and J. Alnis, "Computer modelling of WGM microresonators with a zinc oxide nanolayer using COMSOL multiphysics software," Proc. SPIE **11672**, 1167216 (2021).
27. C. C. Lam, P. T. Leung, and K. Young, "Explicit asymptotic formulas for the positions, widths, and strengths of resonances in Mie scattering," J. Opt. Soc. Am. B **9**, 1585–1592 (1992).
28. S. K. Y. Tang, R. Derda, Q. Quan, M. Lončar, and G. M. Whitesides, "Continuously tunable microdroplet-laser in a microfluidic channel," Opt. Express **19**, 2204–2215 (2011).
29. B. E. A. Saleh and M. C. Teich, *Fundamentals of Photonics*, 2nd ed. (Wiley, 2007).
30. W. Demtröder, *Atoms, Molecules and Photons. An Introduction to Atomic-, Molecular- and Quantum Physics* (Springer, 2010).
31. Q. Ma, T. Rossmann, and Z. Guo, "Temperature sensitivity of silica micro-resonators," J. Phys. D **41**, 245111 (2008).
32. A. C. P. Rocha, J. R. Silva, S. M. Lima, L. A. O. Nunes, and L. H. C. Andrade, "Measurements of refractive indices and thermo-optical coefficients using a white-light Michelson interferometer," Appl. Opt. **55**, 6639–6643 (2016).
33. W. Demtröder, *Laser Spectroscopy* (Springer Berlin Heidelberg, 2008), Vol. **I**.
34. K. Bluss, A. Atvars, I. Brice, and J. Alnis, "Broadband Fabry-Pérot resonator from Zerodur for laser stabilisation below 1kHz linewidth with < 100 Hz/s drift and reduced sensitivity to vibrations," Latv. J. Phys. Tech. Sci. **52**, 11–20 (2015).
35. R. W. Boyd, *Nonlinear Optics*, 4th ed. (Academic, 2020).
36. M. Pollnau and M. Eichhorn, "Spectral coherence, Part I: passive-resonator linewidth, fundamental laser linewidth, and Schawlow-Townes approximation," Prog. Quantum Electron. **72**, 100255 (2020).
37. J. Heebner, V. Wong, A. Schweinsberg, R. Boyd, and D. Jackson, "Optical transmission characteristics of fiber ring resonators," IEEE J. Quantum Electron. **40**, 726–730 (2004).
38. M. Hammer, K. R. Hiremath, and R. Stoffer, "Analytical approaches to the description of optical microresonator devices," AIP Conf. Proc. **709**, 48–71 (2004).
39. K. Okamoto, *Fundamentals of Optical Waveguides* (Elsevier, 2006).
40. A. Yariv, "Critical coupling and its control in optical waveguide-ring resonator systems," IEEE Photon. Technol. Lett. **14**, 483–485 (2002).